

# THE LIFT DEFICIENCY MATRIX OF A HOVERING HELICOPTER ROTOR

Aviv Rosen

Faculty of Aerospace Engineering  
Technion-Israel Institute of Technology  
Haifa 32000, Israel

## Abstract

In the case of a multi-bladed rotor the lift deficiency function is replaced by a lift deficiency matrix (LDM). The elements of the LDM describe inter-blade aerodynamic influences. In the present paper the influence of various parameters on the elements of the LDM is investigated. These parameters include: The ratio between the frequency of perturbations and the rotor angular speed, the number of blades, various physical effects, thrust coefficient and details of the modeling. It is shown that inter-blade influences are strong and using an equivalent single blade representation instead of an accurate multi-blade modeling, may lead to errors.

## List of Symbols

- $c(r)$  - The chord of cross-section  $r$ .  
 $C_T$  - The thrust coefficient of the rotor.  
 $\{D_a(r_c)\}, \{D_e(r_c)\}$  - Vectors defined by Eqs. (3) (4).  
 $D_a(m, r_c), D_e(m, r_c)$  - The perturbations in the normal flow acceleration and velocity, as seen by observers at the mid and three-quarters chordwise points, respectively, at the representative cross-section of blade  $m$ .  
 $[I_{N_b}]$  - A unit matrix of order  $N_b$ .  
 $k$  - Frequency ratio, defined by Eq. (1).  
 $[L_D(r_c, k)]$  - The Lift Deficiency Matrix (LDM).  
 $L_D(r_c, k, m, n)$  - The elements of the Lift Deficiency Matrix.  
 $\tilde{L}(m, r_c)$  - The complex amplitude of the perturbation in the lift force per unit blade length, at the cross-section  $r_c$  of blade  $m$ .  
 $m, n$  - Indices of the blades' numbers.  
 $N_b$  - The number of blades.  
 $R$  - The radius of the rotor.  
 $r_c$  - The radial distance of the representative cross-section.  
 $\rho^*$  - The air mass density.  
 $\chi$  - Nondimensional half chord at the representative cross-section, see Eq. (6).  
 $\sigma$  - The rotor solidity.  
 $\Omega$  - Rotor angular speed.  
 $\omega$  - The frequency of the harmonic perturbations in the rotating system.

## 1. Introduction

The lift deficiency function is a very important and useful tool in the unsteady aerodynamic analysis of oscillating fixed and rotary wings. This function defines the influence of unsteady effects on the magnitude and phase-lag of the lift force.

The lift deficiency function was first defined for fixed wings and later on adapted for the more complicated case of rotary wings. Loewy (Ref. 1) calculated the lift deficiency function of a hovering rotor using a two-dimensional approximate model that takes into account only shed vortices. His model included the effects of the: number of blades, ratio of oscillatory frequency to the angular rotor speed and the inflow ratio. Loewy presented plots of the lift deficiency function and showed that the ratio of oscillatory frequency to the angular rotor speed has a large influence.

Miller (Ref. 2) calculated the oscillatory components of the loads that act on the rotor blades, for harmonics of the rotor frequency. He presented a three-dimensional lifting-line approximate model that took into account trailing and shed vortices. His results indicate that including the influence of trailing vortices may be important.

Dinyavari and Friedmann (Refs. 3,4) used a two-dimensional staggered cascade theory in order to calculate the lift deficiency function of a rotor. It was found that the cascade wake model predicts somewhat larger unsteady aerodynamic effects at integer frequency ratios, than Loewy's theory.

Milliken and Duffy (Ref. 5) calculated the lift deficiency functions for rotors using the pulse transfer technique, that uses discrete vortex filament modeling to represent the time history of the shed vorticity in the wake. The lift response was determined and fast Fourier Transform (FFT) was used to invert the pulse response and obtain the frequency response.

Peters and He (Ref. 6) presented a theory of unsteady aerodynamics for a lifting rotor in hover and forward flight. The theory implicitly includes both dynamic-inflow theory and near wake approximation to the Theodorsen function. The authors calculated the lift deficiency function for different cases and compared it with the results of other theories.

During the last few years a new unsteady aerodynamic model of a hovering rotor, or a rotor in axial flight, was developed in the Technion (Refs. 7-10). This model, named TEMURA (TEchnion Model of Unsteady Rotor Aerodynamics), includes the influences of trailing, shed and bound vortices, together

with geometric effects. This model has been very successful in matching various experimental results and explaining various phenomena (Refs. 10-13).

It was pointed out in (Refs. 7-10) that in the general case of rotary wings, the lift deficiency function should be replaced by a Lift Deficiency Matrix (LDM). This is a square matrix of order  $N_b$ , where  $N_b$  is the number of blades. The elements of this matrix are functions of the rotor geometry, mode of operation and the frequency of the blades' oscillations. The elements of this matrix present the unsteady aerodynamic influence of each blade on itself or on the other blades of the same rotor.

In the present paper the LDM of a hovering rotor will be investigated. The influence of the various effects, various parameters and details of the modeling, on the elements of the LDM will be studied and discussed.

## 2. Theoretical Background

The unsteady aerodynamic model is described in detail in Refs. 8-10 and 14. Here only a brief description, that is necessary for the completeness of the paper, will be presented.

The rotor includes  $N_b$  identical high aspect ratio blades that are uniformly spread over the disk. It is assumed that the lead-lag motions are small enough that variations in the angular spacing between various blades can be neglected. The rotor rotates with a constant angular speed  $\Omega$ .

The model deals with perturbations in the blades' motion about a basic state of hovering. The behavior of all the blades in the basic state is identical and time independent, for an observer rotating with the rotor. It is assumed that the circulation is constant along the blade. Thus the wake behind each blade, in the basic state, is comprised of two trailing vortex filaments: a tip vortex and a root vortex. Since in reality the wake behind every blade rolls up into a concentrated root and tip vortices, this presentation of the wake is good in general. Any geometry of the root and tip vortices in the basic state can be taken into account, including contraction and changes in the axial velocity along the filaments.

TEMURA (TEchnion Model of Unsteady Rotor Aerodynamics) deals with the unsteady aerodynamic loads that act on the blades as a result of small perturbations in their motion (about the basic state). As is common in most unsteady aerodynamic models, harmonic perturbations are considered, having a frequency  $\omega$  in the rotating frame of reference. The unsteady aerodynamic phenomena are largely influenced by the frequency ratio  $k$ :

$$k = \omega / \Omega \quad (1)$$

The perturbations in the motions of the blades result in the following aerodynamic perturbations:

- a) Perturbations in the aerodynamic loads that act on the blades that present perturbations in the circulations of the bound vortices.
- b) Perturbations in the intensity of the circulation of the trailing vortices that are superimposed on the circulation of the trailing vortices in the basic state.
- c) Shed vortices that form helical surfaces of vortices below the rotor plane.

A representative cross-section for each blade is defined. It is located at a radial distance  $r_c$ . Usually the three-quarters cross-section is chosen as the representative one, namely  $r_c = 0.75 R$ , where  $R$  is the rotor radius.

Since a linear model is considered, all the perturbations have the same frequency  $\omega$ . It is convenient to describe all the perturbation amplitudes as complex numbers. The complex amplitude of each perturbation represents magnitude and phase angle shift.

$\tilde{L}(m, r_c)$  is the complex amplitude of the perturbation in the lift force per unit length, at the cross-section  $r_c$  of the  $m^{\text{th}}$  blade.  $\tilde{L}(r_c)$  is a vector of order  $N_b$  that describes the perturbations of the lift forces at the cross-sections  $r_c$  of all the blades:

$$\left\{ \tilde{L}(r_c) \right\} = \left[ \tilde{L}(1, r_c), \dots, \tilde{L}(m, r_c), \dots, \tilde{L}(N_b, r_c) \right]^T \quad (2)$$

The perturbation in the motion of cross-section  $r_c$  of blade  $m$ , is defined by the following two variables:

- a) A perturbation in the normal component of the incoming velocity as seen by an observer at the three-quarters chord point of cross-section  $r_c$  of blade  $m$ , denoted  $D_e(m, r_c)$ .
- b) A perturbation in the normal component of the acceleration of the incoming flow, as seen by an observer at the mid-point of cross-section  $r_c$  of blade  $m$ , denoted  $D_a(m, r_c)$ .

The above two contributions include the influence of perturbations in the motion of the blade, as well as the influence of geometric effects (perturbations in the wake geometry).

It is convenient to define two vectors,  $D_e(r_c)$  and  $D_a(r_c)$ , that describe the perturbation in the incoming flow as seen by observers at the cross-sections  $r_c$  of all the blades:

$$\left\{ D_e(r_c) \right\} = \left[ D_e(1, r_c), \dots, D_e(m, r_c), \dots, D_e(N_b, r_c) \right]^T \quad (3)$$

$$\left\{ D_a(r_c) \right\} = \left[ D_a(1, r_c), \dots, D_a(m, r_c), \dots, D_a(N_b, r_c) \right]^T \quad (4)$$

The relations between the perturbations in the cross-sectional lift forces, and the perturbation in the motions of the blades relative to the fluid, is given by the following equation:

$$\{\tilde{L}(r_c)\} = -2\pi \dot{\rho} \Omega r_c^2 \chi ([I]_{N_b} \{D_a(r_c)\} + [L_D(r_c, k)] \{D_e(r_c)\}) \quad (5)$$

$\dot{\rho}$  is the air mass density.  
 $\chi$  is a nondimensional half chord of the cross-section  $r_c$ , defined as:

$$\chi = c(r_c) / (2r_c) \quad (6)$$

$c(r)$  is the chord at cross-section  $r$ .

$[L_D(r_c, k)]$  is the lift deficiency matrix (LDM). This is a square, complex nondimensional matrix of order  $N_b$ . Because of simple physical reasoning, that is also supported by mathematical derivations, there exists a certain circular pattern of the matrix  $[L_D(r_c, k)]$ . Namely, all the elements  $(m, m+i)$ , for a certain constant value of  $i [0 \leq i \leq (N_b - 1)]$ , are identical for any  $m$  in the range  $1 \leq m \leq N_b$ . If  $(m+i) > N_b$ , then  $(m+i)$  is replaced by  $(m+i - N_b)$ . Matrices that exhibit this special circular pattern are called circulants. The properties of these matrices are described in Ref. 15. The LDM is a function of the choice of the representative cross-section,  $r_c$ , and frequency ratio,  $k$ .

The contributions associated with  $\{D_a(r_c)\}$  are known otherwise as the noncirculatory or added-mass contributions. They are usually very small and thus of little interest. The contributions associated with  $\{D_e(r_c)\}$  are the circulatory ones, and are the subject matter of this paper. They depend on the LDM.

In what follows the elements of the matrix  $[L_D(r_c, k)]$  will be investigated. These elements are denoted  $L_D(r_c, k, m, n)$ , where  $1 \leq m, n \leq N_b$ . Since the matrix is a circulant, it is sufficient to consider only a single row. In what follows the first row will be considered.

### 3. The Influence of the Number of Blades

In this section the influence of the number of blades on the LDM is investigated. While changing the number of blades, the rotor solidity ( $\sigma$ ) and the thrust coefficient ( $C_T$ ) will be kept constant, having typical values of  $C_T = 0.00510$  and  $\sigma = 0.0821$ .

Three kinds of results will be presented:

- A complete model that includes all the unsteady effects.
- A model that includes perturbations in the bound vortices of the other blades and perturbations in all the trailing vortices, but does not include the shed vortices in the far field. This model will be denoted (bound+trail.).
- A model that includes perturbations in the bound vortices of the other blades and shed vortices, but

does not include perturbations in the trailing vortices. It will be denoted (bound + shed).

It should be noted that all the three models include the near field (see Refs. 8-10 and 14), namely the bound vortices of the blade itself and the shed vortices near its trailing edge.

The three kinds of results will help in studying the relative influence of perturbations in the trailing or shed vortices. It was found that the influence of perturbations in the bound vortices of the other blades is very small and thus will not be studied separately.

Unless indicated otherwise,  $r_c = 0.75 R$ , and the wake geometry includes contraction and variations in the axial induced velocity along the wake as described in Ref. 10.

The real and imaginary parts of the elements of the LDM will be shown as functions of the frequency ratio  $k$ .

#### 3.1 A single blade ( $N_b=1$ )

The lift deficiency of a single blade is shown in Fig. 1.

The real part is larger than the imaginary one, therefore it will practically define the amplitude of the lift perturbation. The real part has maxima at approximately  $k=n+0.5$ , where  $n$  is any integer number. At  $k=0.5$  the maximum value is larger than 1.3. As  $k$  is increased the maxima values decrease as well as the sharpness of this maxima. Also as  $k$  increases the maxima occur at  $k$  values that are higher than  $(n+0.5)$  and the differences increase with  $k$ . It can be shown that near  $k$  values of  $(n+0.5)$  the vorticity structure at the wake layers below the blade is opposite in phase to the vorticity structure just behind the blade. Thus while the vortices behind the blade tend to reduce the magnitude of variations in the lift, namely give amplitude values lower than unit, the vortices in the wake layers below the rotor tend to increase the variations of these forces. It turns out that the resultant influence of the layers below the rotor is stronger than the influence of the vortices just behind the blade, therefore the perturbations in the lift force are increased, namely the lift deficiency amplitudes are larger than unit.

There are minima of the real part near integer values of  $k$ . As  $k$  increases the trends concerning the minima are similar to those concerning the maxima, that were indicated above. It can be shown that near integer values of  $k$  the vorticity structure at the wake layers below the blade is identical to that of the wake just behind the blade. Thus the trend of reducing the perturbations in the aerodynamic loads is increased and therefore minima are obtained.

The imaginary part exhibits relatively sharp variations near the maxima of the real part, with slightly less sharp variations near its minima. The imaginary part oscillates at the same frequency as the real part, namely a period (when  $k$  is considered) of 1.

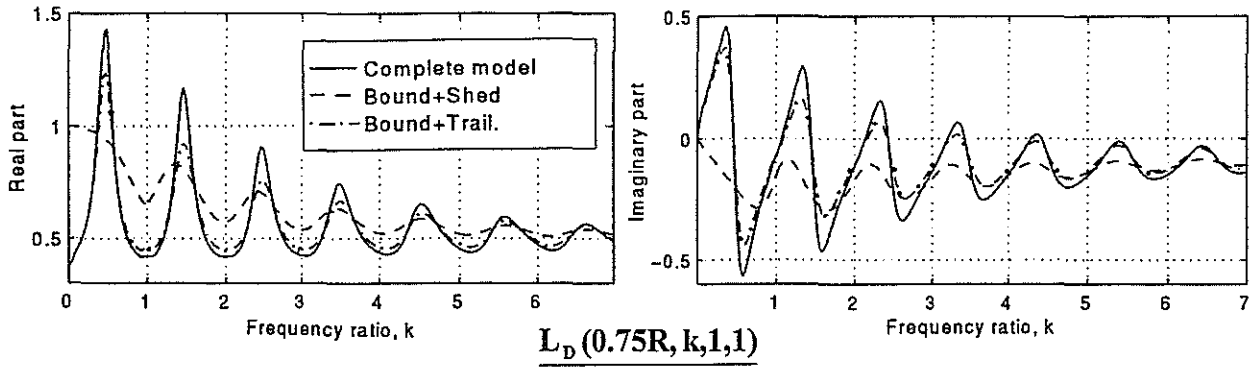


Fig. 1. The Lift Deficiency in the case of a single blade.

At low values of  $k$  the imaginary part exhibits absolute values that exceed 0.5. The absolute values of the imaginary part decrease rapidly as  $k$  increases.

For large values of  $k$  the real part converges to 0.5 while the imaginary part obtains small negative values, identical trend appears in the case of the classical lift deficiency function of Theodorsen. This indicates that at high frequency ratios, as expected from physical reasoning, the near wake starts to dominate the phenomenon.

The perturbations in the circulation of the trailing vortices have the largest influence. When shed vortices in the far field are neglected (bound+trail.) the results are very similar to the complete model, with significant differences only near the maxima and minima of the real and imaginary parts (the differ-

ences in the case of the minima of the real part are relatively small).

If the influence of perturbations in the circulations of the trailing vortices is neglected and only the influence of shed vortices is considered, the results show large differences in comparison with the complete model.

### 3.2 A two bladed rotor ( $N_b=2$ )

There are two elements in each row of the LDM, that are presented in Fig. 2. The influence of a blade on itself will be considered first, namely  $L_D(0.75 R, k, 1, 1)$ . Then the influence of a blade on its neighbor will be studied, namely  $L_D(0.75 R, k, 1, 2)$ .

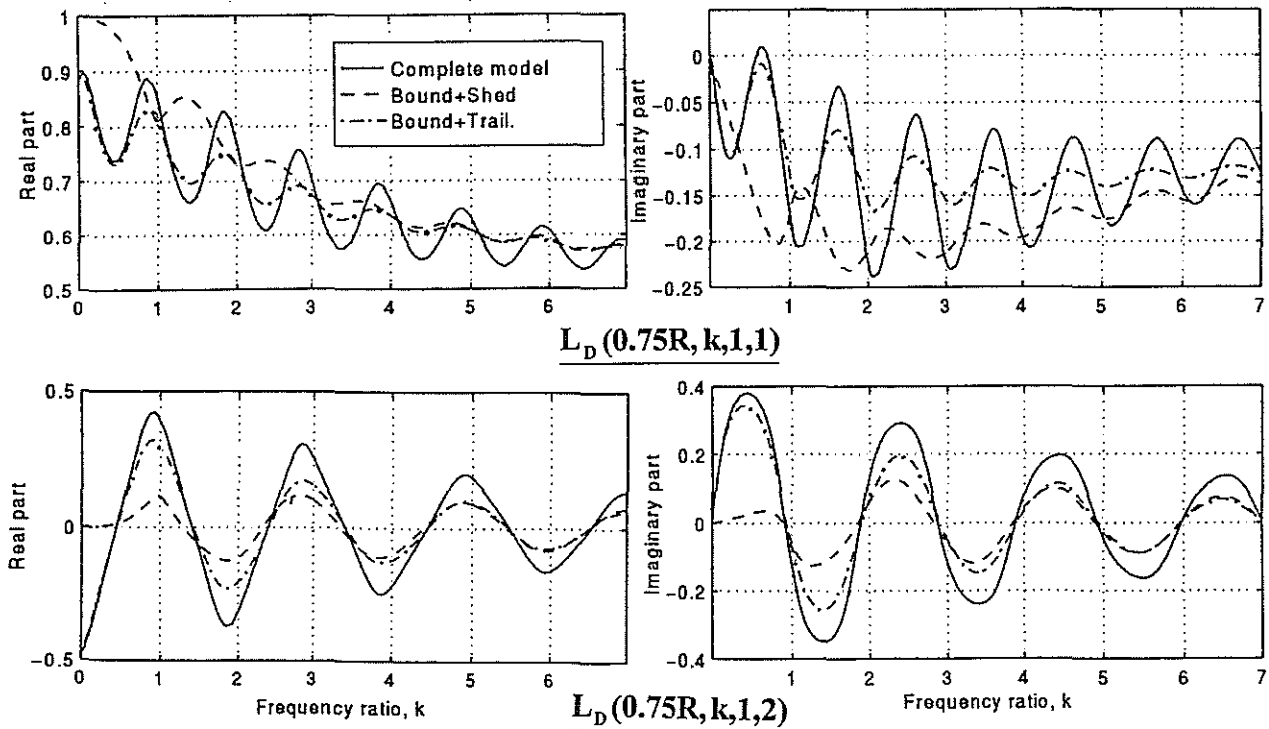


Fig. 2. The Lift Deficiency Matrix in the case of a two bladed rotor.

$L_D(0.75 R, k, 1, 1)$  exhibits a drastic difference when compared with the same term of a single-bladed rotor, Fig. 1. There is a reduction in the magnitude of the real and imaginary parts. The real part remains the larger one, but it is always smaller than unit. The imaginary part is always negative and larger than  $-0.25$ , except for very small positive values between  $k=0.6$  and  $0.8$ . The real part exhibits minima near  $k=n+0.5$  and maxima near integer values of  $k$ , exactly opposite to the case of a single bladed rotor. While in the case of a single bladed rotor the exact location of the extremums is shifted to the right as  $k$  is increased, in the case of a two bladed rotor the shift is to the left. Also the imaginary part of  $L_D(0.75, k, 1, 2)$  shows an opposite behavior to that of the imaginary part of the same term in the case of a single bladed blade, where maxima replace minima and vice versa.

The reason for this drastic change in the influence of the blade on itself, is the presence of a second blade. It should be noted that  $L_D(r_c, k, 1, 1)$  represents perturbations in the lift of the first blade due to perturbations in the normal velocity seen by this blade. Yet there is a large influence of the presence of the second blade, even if it is "static" and does not "perform perturbations of its own". This behavior is explained below. Assume that only the first blade exhibits perturbations about the basic state. This will result in variations in the circulation along the blade and in the vorticity distribution over the wake (trailing and shed vortices) behind it. These variations (especially in the wake) will lead to variations in the velocities that are induced along the second blade, and in return variations in the lift force and circulation along the second blade. The last variations will result in variations in the wake behind the second blade. The wake of the second blade is closer to the first blade than its own wake, when both of them pass below it. Thus variations in the vorticity distribution in the wake of the second blade have a stronger influence on the first blade, than similar variations in the wake of the first blade itself. This is the reason for the drastic change in  $L_D(0.75 R, k, 1, 1)$  as a result of adding another blade.

The above discussion shows that the presence of a second blade changes the entire phenomenon. The idea of replacing a multi-bladed rotor by an equivalent single-bladed rotor, when unsteady aerodynamics is considered, may lead to errors in many cases.

As in the case of a single bladed rotor, a model that does not include shed vortices (bound+trail.) exhibits a very similar behavior to the complete model, with large differences in the values of the real and imaginary parts at the maxima or minima.

The trends shown by the model that does not include trailing vortices (bound+shed) are different from those of the complete model (unlike the case of a single blade). In general the maxima in the real and

imaginary parts are replaced by minima, and vice versa. In addition, the average value of the real part in this case (bound+shed) is larger than that of the real part of the complete model and smaller (more negative) when it comes to the imaginary part.

Now the influence of perturbations in the normal velocity seen by the second blade, on the lift force of the first blade, will be investigated, namely the element  $L_D(0.75 R, k, 1, 2)$ .

The real and imaginary parts of the second element of the LDM exhibit oscillations about zero, as  $k$  varies. The nondimensional period of these oscillations equals approximately 2, as compared to 1 in the case of  $L_D(0.75 R, k, 1, 1)$ . It can be shown that there is a difference of 2 in  $k$  between two consequent cases where the vorticity distribution in the returning wake is identical or opposes the vorticity distribution behind the blade itself.

The amplitudes of the oscillations in the real and imaginary parts of  $L_D(0.75 R, k, 1, 2)$  are approximately of the same order-of-magnitude. They decrease as  $k$  increases and exhibit a phase difference, when the variation with  $k$  is considered, of approximately a quarter of a period, namely 0.5. The models (bound+trail.) and (bound+shed), exhibit a behavior that is almost identical to that of the complete model concerning the oscillatory variation with  $k$ , but differ in the amplitude of the oscillations. At low frequency ratios,  $k \leq 3$ , the model without trailing vortices shows much smaller amplitudes, while the model without shed vortices (bound+trail.) exhibits better agreement with the complete model. At higher values of  $k$  the incomplete models agree nicely between themselves, but still show lower amplitudes than the complete model.

### 3.3 A four bladed rotor ( $N_b=4$ )

In this case there are four different elements of the LDM that are presented in Fig. 3.

Comparison between  $L_D(0.75 R, k, 1, 1)$  for  $N_b = 2$  and  $N_b = 1$  shows that the amplitude of the oscillations of the real and imaginary parts decrease as  $N_b$  is increased. This trend continues for  $N_b = 4$ , where the real and imaginary parts show only small oscillations about their mean values. The mean value of the real part, at a certain high value of  $k$ , increases as  $N_b$  increases (for  $k=7$  it is less than 0.6 for  $N_b = 2$ , and 0.67 for  $N_b = 4$ ). The same trend appears in the imaginary part.

The model that does not include shed vortices (bound+trail.) gives results that are very close to the complete model. The other model (bound+shed) exhibits larger differences.

The influence of the second blade on the first one,  $L_D(0.75 R, k, 1, 2)$ , exhibits an oscillatory behavior that is somewhat similar to that of the same element in the case of a two bladed rotor, but the period of

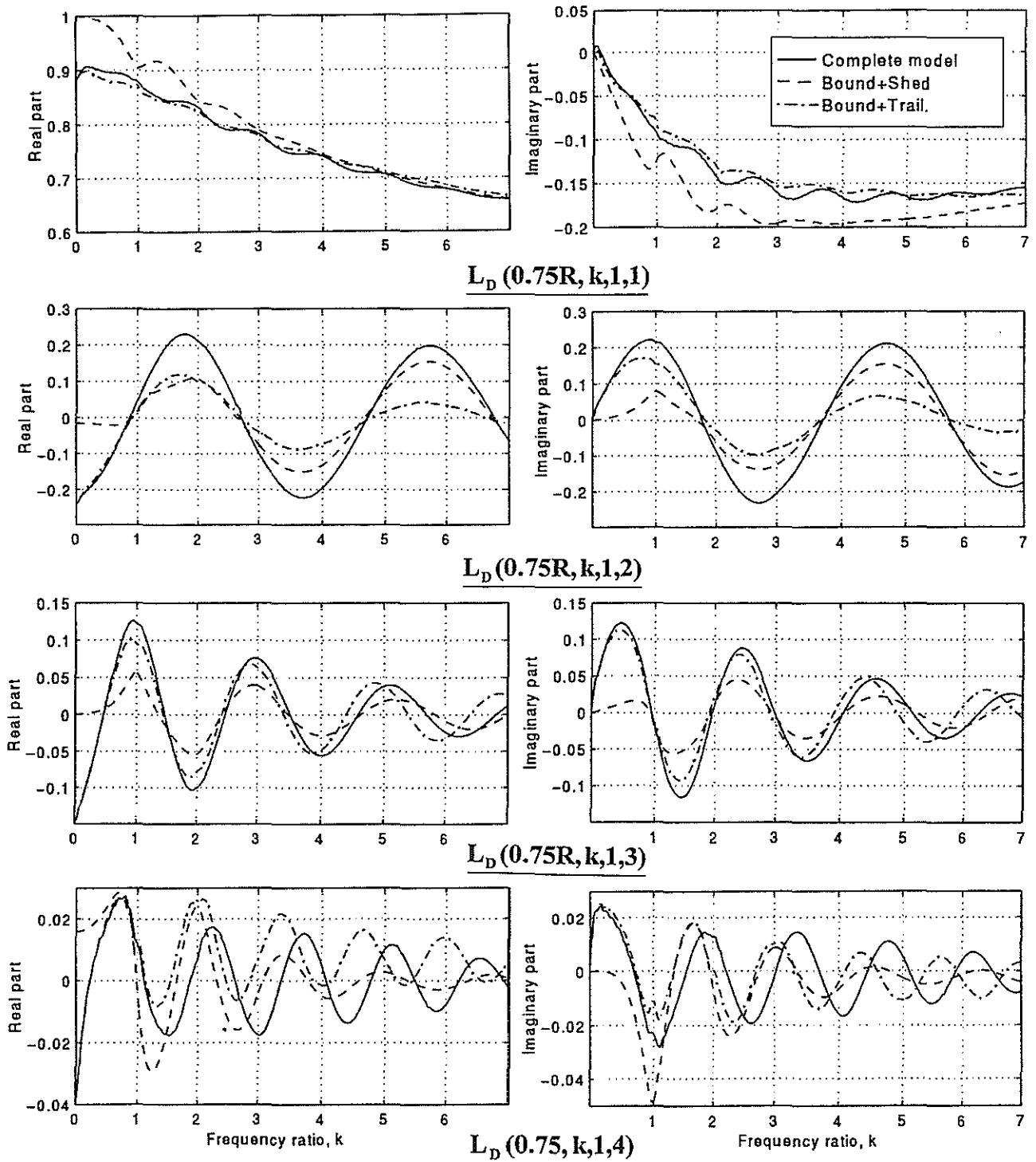


Fig. 3. The Lift Deficiency Matrix in the case of a four bladed rotor.

oscillation with  $k$  increases from 2 in the case of  $N_b = 2$ , to 4 in the case of  $N_b = 4$ . Again the amplitudes of the real and imaginary parts of the complete model are similar, but appear with a phase difference between them (with respect to  $k$ ) of approximately 1 (quarter of a period). At low values of  $k$  ( $k \leq 2$ ) the model that does not include shed vortices (bound+trail) shows better agreement with the complete model, than the (bound+shed) model. At higher values of  $k$  the trends change and the model (bound

+shed) exhibits better agreement with the complete model than the model (bound+trail).

The influence of one blade on the other decreases as the angular spacing between them increases, this can be seen when  $L_D(0.75 R, k, 1, 3)$  and  $L_D(0.75 R, k, 1, 4)$  are examined. They oscillate about zero, but the period varies from 2 for  $L_D(0.75 R, k, 1, 3)$ , to 1.5 for  $L_D(0.75 R, k, 1, 4)$ . There is a phase shift of approximately a quarter of a period between the oscillations of the real and

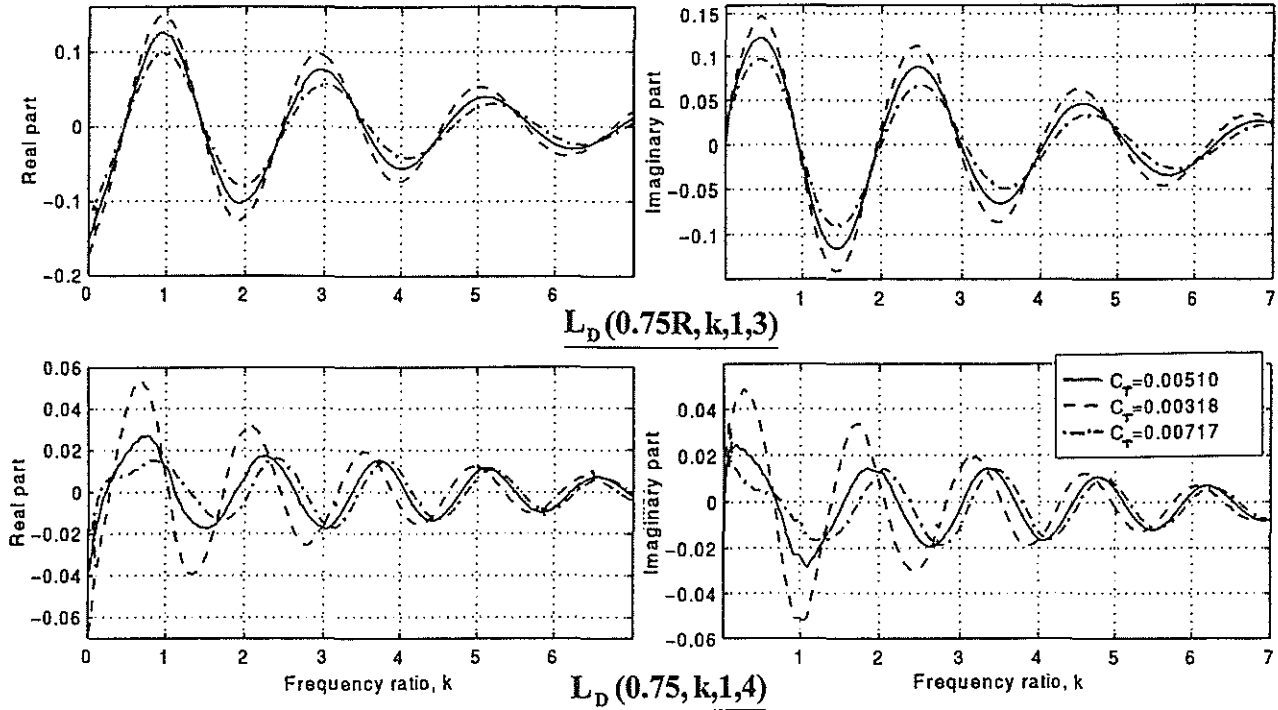


Fig. 4. The influence of the thrust coefficient on the Lift Deficiency Matrix ( $N_b=4$ ).

imaginary parts. At low values of  $k$  the model (bound+trail) exhibits a relatively good agreement with the complete model, while there are large differences in the case of (bound+shed). At higher values of  $k$  both models exhibit relatively large differences when compared with the complete model.

#### 4. The Influence of the Thrust Coefficient

Changing the rotor thrust changes the basic induced velocity through the rotor and thus changes the wake geometry and in particular the distances between the vortex elements in the wake and the blades. Increasing the thrust will increase the basic induced velocity and as a result increase the above mentioned distances and thus reduce the perturbations in the induced velocities. Therefore, as a result of increasing the thrust the unsteady effects will decrease. An opposite trend is expected when the thrust is decreased.

In Fig. 4 the influence of thrust variations on the four bladed rotor are presented. In addition to the nominal case of  $C_T = 0.00510$ , two other cases, where  $C_T$  is equal to 0.00318 and 0.00717, are shown.

The influence of the thrust variations on  $L_D(0.75R, k, 1, 1)$  and  $L_D(0.75, k, 1, 2)$  are practically negligible and therefore are not presented. In the case of  $L_D(0.75R, k, 1, 3)$  there are variations in the magnitude of maxima and minima of the real and imaginary parts that exceed 20%. As expected there is an in-

crease in the amplitude of the LDM element when  $C_T$  decreases, and a decrease when  $C_T$  increases.

In the case of  $L_D(0.75R, k, 1, 4)$  the influences of the thrust variations are larger. The amplitudes of the maxima and minima of the real and imaginary parts are doubled at low values of  $k$  as a result of decreasing  $C_T$ . Moreover, there is also a shift in the location of the maxima and minima.

#### 5. The Influence of the Wake Geometry

In the above examples the wake geometry was identical to the geometry that was described in Ref. 10. In what follows this model is denoted wake model no. 3. In order to check the sensitivity of the results to the wake geometry, two other models were used:

- A cylindrical model where there is no contraction and the wake moves downward with the average induced velocity at the disc, that is equal to  $\sqrt{C_T}/2$ .

To be denoted wake model no. 1 in what follows.

- A wake geometry according to Landgrebe (Ref. 16) to be denoted wake model no. 2.

A comparison between the lift deficiency elements when using the three wake models, is presented in Fig. 5.

In the case of  $L_D(0.75, k, 1, 1)$  the results of wake models 1 and 2 oscillate about the results of model 3. The amplitudes of the oscillations decrease as  $k$  increases. The cylindrical wake (wake 1) exhibits larger oscillations than Landgrebe's model (wake 2). The

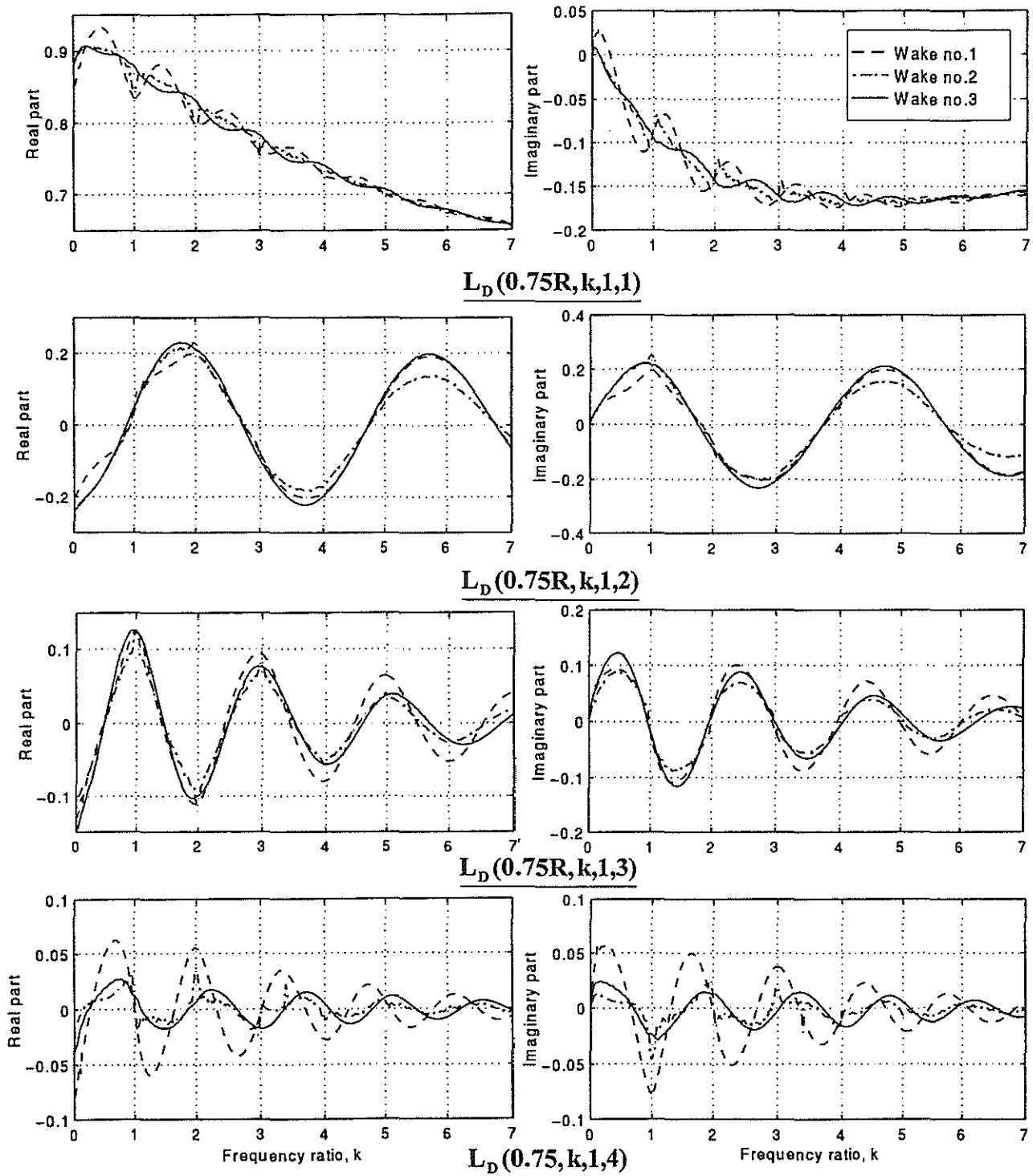


Fig. 5. The influence of the wake geometry on the Lift Deficiency Matrix ( $N_b=4$ ).

oscillations of wake model 2 are characterized by sharp extremums near integer values of  $k$ .

In the case of the influence of the second blade on the first one,  $L_D(0.75R, k, 1, 2)$ , wake model 2 agrees nicely with wake model 3 at low frequency ratios ( $k < 2.5$ ), while wake model 2 exhibits larger differences when compared with model 3. At higher frequency ratios the trend reverses, namely models 1 and 3 agree nicely, while model 2 exhibits significant differences that exceed 30% for the real part at  $k=5.5$ .

For  $L_D(0.75R, k, 1, 3)$  there is in general a better agreement between wake models 2 and 3, than between wake model 1 and the other two, yet there are frequency ratios where models 1 and 3 exhibit better agreement. The differences exceed 50% at high  $k$  values.

As in the case of the thrust coefficient influences, the influence of the fourth blade on the first one,  $L_D(0.75R, k, 1, 4)$ , is the smallest one, but the most



sensitive to variations. There are relatively small differences between wake models 2 and 3 except for integer values of  $k$  where model 2 exhibits the previously mentioned sharp extremums, while there are larger differences between these two and the cylindrical wake model (wake 1). These differences exceed 100% in amplitude (compared to wake model 3) and large shifts in the locations of extremums can be seen.

### 6. The Influence of the Location of the Representative Cross-Section

In all the above results the representative cross-section was chosen as  $0.75R$ . In Fig. 6 the elements of the LDM of a four-bladed rotor using two other locations,  $r_c = 0.70R$  and  $r_c = 0.80R$ , are compared with the results for  $r_c = 0.75R$ .

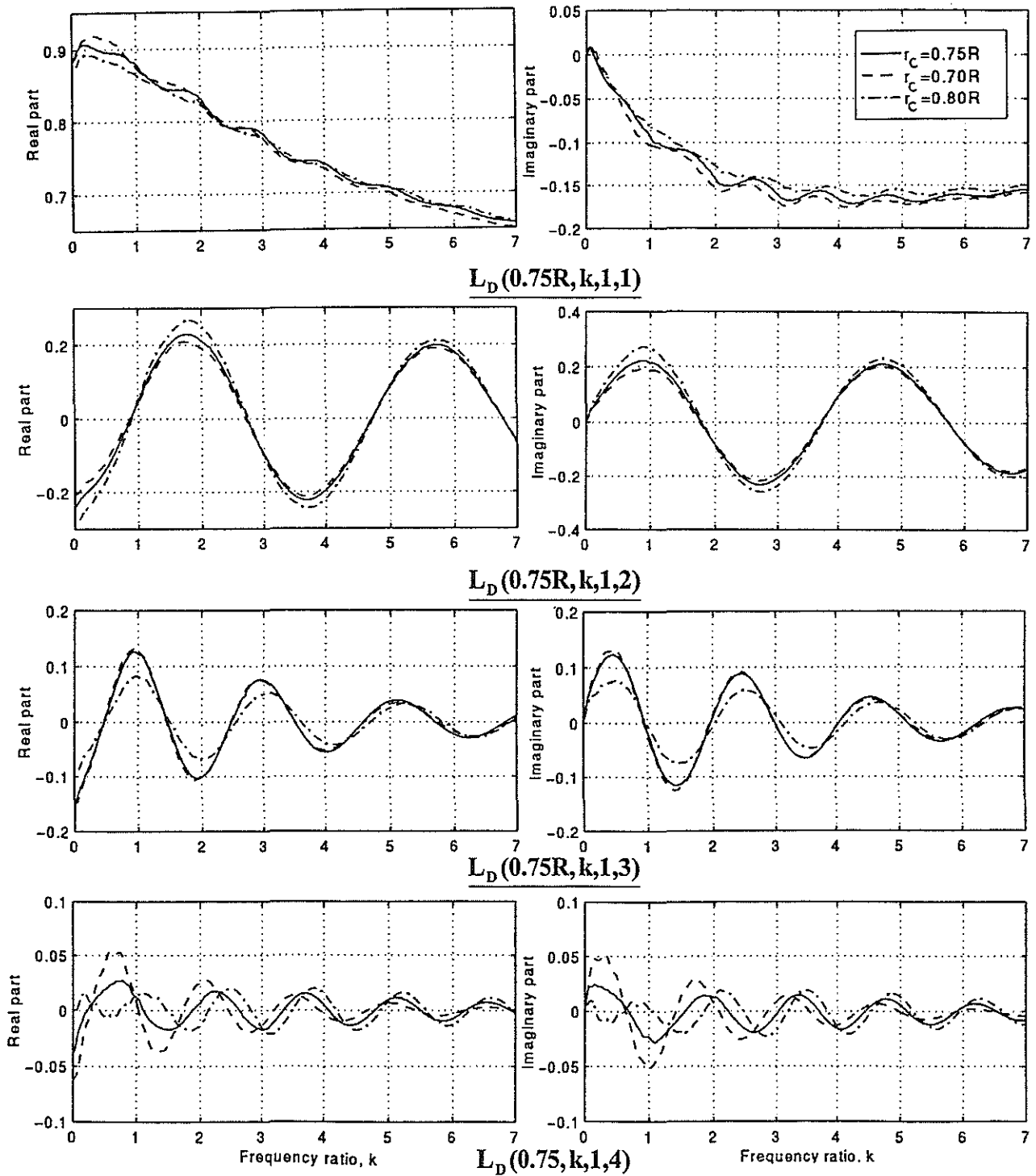


Fig. 6. The influence of the location of the representative cross-section on the Lift Deficiency Matrix ( $N_b=4$ ).

In the case of  $L_D(0.75R, k, 1, 1)$  and  $L_D(0.75R, k, 1, 2)$  the influence of  $r_c$  is relatively small.

For  $L_D(0.75R, k, 1, 3)$  there are very small differences between  $r_c = 0.75R$  and  $r_c = 0.7R$ , while at low  $k$  values there are differences in amplitude between  $r_c = 0.75R$  and  $r_c = 0.8R$  that exceed 35%.

Similar to the previous results,  $L_D(0.75R, k, 1, 4)$  is the most sensitive to  $r_c$  variations. There are large variations in amplitude (that exceed 100%) and also large variations in the location of the extremum points.

## 7. Conclusions

In the case of a multibladed rotor there are strong inter-blade aerodynamic interactions. For unsteady aerodynamic analysis these interactions are conveniently described by the Lift Deficiency Matrix (LDM). An attempt to replace this matrix by a lift deficiency function for an "equivalent" rotor having a single blade, may lead to significant errors and an incapability to simulate important phenomena.

The lift deficiency matrix depends strongly on the number of blades and the frequency ratio, namely the ratio between the frequency of the perturbation in the rotating frame of reference and the rotor angular speed. The perturbations in the vorticity distribution of the trailing vortices and the shed vortices behind the blades, have a strong influence on the elements of the lift deficiency matrix. At low frequency ratios the influences of the perturbations in the trailing vortices have much stronger influences, therefore ignoring their influence may lead to large errors.

The wake geometry influences the LDM elements. It is important to consider contraction of the wake and variations of the axial induced velocity along the wake. The thrust coefficient influences the wake geometry and thus influences the LDM.

There is a small sensitivity of the LDM to the location of the representative cross-section. It is recommended to take the "classical" value of  $r_c = 0.75R$ .

For four bladed rotors the influence of the fourth blade on the first one is the weakest, yet it is the most sensitive to variations in the model and the parameters.

Acknowledgment - The author would like to thank Mr. J. Goldin and Mrs. R. Yaffe for their help with the numerical work. He would also like to thank Mrs. A. Goodman for typing the paper.

## References

1. Loewy, R.G., "A 2-D Approximation to the Unsteady Aerodynamics of Rotary Wings", *J. of Aero. Sci.*, **24**, 1957, pp. 81-92.
2. Miller, R.H., "Rotor Blades Harmonic Air Loading", *AIAA J.*, **2**, 1964, pp. 1254-1269.
3. Dinyavari, M.A.H. and Friedmann, P.P., "Unsteady Aerodynamics in Time and Arbitrary Motion of Rotary Wings in Hover and Forward Flight", AIAA Paper 84-0988, 1984.
4. Dinyavari, M.A.H. and Friedmann, P.P., "Time Domain Unsteady Incompressible Cascade Airfoil Theory for Helicopter Rotors in Hover", *AIAA J.*, **27**, 1989, pp. 257-267.
5. Milliken, R.L. and Duffy, R.E., "Lift Deficiency Functions for Aspect Ratio 6, 12 and 18 Rotor Blades from Advance Ratios of 0 to 0.4", AIAA paper 88-4494, 1988.
6. Peters, D.A. and He, C.J., "A Closed-Form Unsteady Aerodynamic Theory for Lifting Rotors in Hover and Forward Flight", Proc. of the American Helicopter Soc. 43rd Forum, 1987, pp. 839-865.
7. Iosilevskii, G., "Model for Non-Stationary Aerodynamics of Rotary Wings in Axial Flight", D.Sc. Thesis (in Hebrew), Faculty of Aerospace Eng., Technion, Haifa, March 1989, 201 pp.
8. Rosen, A. and Isser, A., "The Influence of Variations in the Locations of the Blades on the Loads of a Helicopter Rotor During Perturbations About an Axial Flight", TAE Report No. 721, Technion, Faculty of Aerospace Eng., Oct. 1994.
9. Isser, A. and Rosen, A., "A Model of the Unsteady Aerodynamics of a Hovering Helicopter Rotor that Includes Variations of the Wake Geometry", *J. of the American Helicopter Society*, **40**, 1995, pp. 6-16.
10. Rosen, A. and Isser, A., "A New Model of Rotor Dynamics During Pitch and Roll of a Hovering Helicopter", *J. of the American Helicopter Society*, **40**, 1995, pp. 17-28.
11. Rosen, A., Isser, A. and Yoshpe, M., "The Influence of Unsteady Aerodynamics and Inter-Blade Aerodynamic Coupling on the Blades Response to Harmonic Variations of Their Pitch Angles", *Aeronautical J.*, **100**, 1996, pp. 27-35.
12. Rosen, A. and Isser, A., "The Influence of Unsteady Aerodynamic Effects on the Coupled Free Vibrations of Rotor Flapping and Body Pitch and Roll in Hover", *J. of the American Helicopter Society*, **41**, 1996, pp. 208-218.
13. Isser, A. and Rosen, A., "The Pitch Damping of a Hovering Rigid Rotor", *J. of the American Helicopter Society*, **42**, 1997, pp. 96-99.
14. Rosen, A. and Isser, A., "Investigation of the Technion Model of Unsteady Rotor Aerodynamics (TEMURA)", 6th International Workshop on Dynamics and Aeroelastic Stability Modeling of Rotorcraft Systems, The Univ. of California, Los Angeles, CA, Nov. 8-10, 1995.
15. Graybill, F.A., "Matrices with Applications in Statistics", Wadsworth Inc. 1983.
16. Landgrebe, A.J., "The Wake Geometry of a Hovering Helicopter Rotor and Its Influence on Rotor Performance", *J. of the American Helicopter Society*, **17**, 1972, pp. 3-15.